Differentiation of Cation−π Bonding from Cation−π Intermolecular Interactions: A Quantum Chemistry Study Using Density-Functional Theory and Morokuma Decomposition Methods

Weiliang Zhu,[†,‡,§] Xiaojian Tan,[†] Jianhua Shen,*[,†] Xiaomin Luo,[†] Feng Cheng,[†] Puah Chum Mok,*[,§] Ruyun Ji,[†] Kaixian Chen,[†] and Hualiang Jiang*[,†]

Center for Drug Discovery and Design, State Key Laboratory of New Drug Research, Shanghai Institute of Materia Medica, Shanghai Institutes for Biological Sciences, Chinese Academy of Sciences, 294 Taiyuan Road, Shanghai 200031, P. R. China, School of Chemical & Life Sciences, Singapore Polytechnic, 500 Dover Road, Singapore 139651, Singapore, and Technology Centre for Life Sciences, Singapore Polytechnic, 500 Dover Road, Singapore 139651, Singapore

Received: September 24, 2002; In Final Form: January 14, 2003

A strong interaction called cation−π bonding, which we named because it occurs between aromatics and divalent metal cations, has been successfully differentiated from the normal cation−π intermolecular interactions. Our findings were based on the B3LYP/6-311++G(d,p) calculations and Morokuma decomposition analyses on the complexes formed by substituted benzenes with alkaline metal and alkaline earth metal ions. In comparison with the common cation−π intermolecular interaction, the cation−π bond in the complexes of either Be^{2+} or Mg^{2+} with the aromatics has its own characteristics: (a) short bond lengths, (b) very strong binding strength, (c) significant nonelectrostatic interaction that constitutes more than 50% of the total binding strength, (d) obvious cation−π orbital interaction, and (e) special orbital interaction pattern that only the π orbitals of the aromatics interact with the s, p_x, and p_y atomic orbitals of metal cations for forming bonding MOs. While the electrostatic interaction is significantly affected by the nature of the substituents attached to the benzene, the nonelectrostatic interaction and orbital interaction are not. Furthermore, the total binding strength and electrostatic interaction are well correlated with the Hammett electronic parameters. This structural and thermochemical information is highly useful in identifying cation−π bonds. Moreover, they are equally helpful for modifying current force fields in reproducing this unusual chemical bond that is commonly encountered in both chemical and biological systems.

1. Introduction

The interaction between a cation and an aromatic system (cation−π interaction) has been demonstrated by both experimental and theoretical studies in the past.[1] Scientists not only realized the importance of this unusual interaction in chemistry, biological processes, and material science, but also made use of this interaction in designing new drug leads and other new functional materials.[2−18] However, in a majority of these studies, much attention has been paid to the monovalent cations, such as ammonium, tetramethylammonium, and alkaline metal cations.[1,3,7,10,13,16−18] These findings showed that the electrostatic interaction plays a very important role in the binding between the cations and aromatics. For example, in the binding of a monovalent cation with benzene, the percentage of the electrostatic interaction in the overall binding strength is normally higher than 50%, suggesting that the interaction is electrostatic in nature.[1,12,17,19] Moreover, their binding strength is normally not as strong as a chemical bonding.[1,12,17,19] Therefore, this interaction has been assigned as a kind of intermolecular interaction rather than chemical bonding.

In recent years, the cation−π interaction involving a divalent cation was found to play significant roles in a number of biological systems. For example, the alkaline earth metal cation Mg^{2+} is controlled by a tryptophan residue that can be blocked or permeated in the selectivity filter of the *N*-methyl-D-aspartate receptor.[20] Divalent metal cation−π interactions have also been suggested to be involved in DNA bending, DNA−protein recognition, base-flipping, RNA folding, and catalysis.[11] Furthermore, strong evidence pointing to a cation−π binding of Mg^{2+} with HIV integrase was demonstrated.[14] However, only few experimental and theoretical studies on this interaction have been published to date. Generally, those few studies concentrated on demonstrating the existence of the M^{2+}−π interaction or on geometrical parameters and binding strength rather than on binding nature and components.[5,11,14,15] Previously, we carried out a theoretical calculation on the interaction between alkaline earth metal cations and benzene, which is so strong that it should be considered a chemical bond rather than the usual intermolecular interaction.[21] The analysis on the components of the binding energy showed that the electrostatic interaction does not dominate the interaction, suggesting that this interaction might be in nature different from the interaction between monovalent cations and aromatics.[21] But, if it is a chemical bonding, its characteristics remain unclear. This would lead to

* Corresponding authors. Please address correspondence and requests for reprints to Prof. Hualiang Jiang, Shanghai Institute of Materia Medica, Chinese Academy of Sciences, 294 Taiyuan Road, Shanghai 200031, P. R. China. Phone: +86-21-64311833, ext 222. Fax: +86-21-64370269. E-mail: jiang@iris3.simm.ac.cn or hljiang@mail.shcnc.ac.cn.

† Chinese Academy of Sciences.

‡ School of Chemical & Life Sciences, Singapore Polytechnic.

§ Technology Centre for Life Sciences, Singapore Polytechnic.

10.1021/jp0270598 CCC: $25.00
Published on Web 03/08/2003

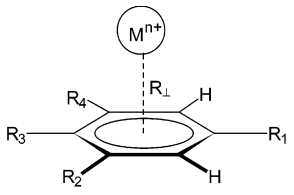

Aromatic 1: R_1=-NH_2, R_2=R_3=R_4=H
Aromatic 2: R_1=-CH_3, R_2=R_3=R_4=H
Aromatic 3: R_1=-OH, R_2=R_3=R_4=H
Aromatic 4: R_1=R_2=R_3=R_4=H
Aromatic 5: R_1=-F, R_2=R_3=R_4=H
Aromatic 6: R_1=R_3=-F, R_2=R_4=H
Aromatic 7: R_1=R_2=R_4=-F, R_3=H.
Cation: M^{n+}=Li^+, Na^+, K^+, Be^{2+}, Mg^{2+} and Ca^{2+}

Figure 1. The complexes formed by substituted benzenes and M^{n+}.

some unanswered questions. First, does the bonding exist between those metal cations and other aromatics? Second, what is the nature of this bonding? And third, how does the atomic orbital interact between the metal cations and aromatics? To answer these questions, we performed a theoretical calculation on the complexes formed by different aromatics and alkaline earth metal cations. The objectives of this study are (a) to explore the importance of the electrostatic and nonelectrostatic interactions to the $M^{2+}-\pi$ binding, (b) to study the geometrical characteristics of $M^{2+}-\pi$ complex, (c) to compare the difference in the binding between $M^+-\pi$ and $M^{2+}-\pi$, (d) to testify how the substitutes will impact the binding between M^{2+} and π, and (e) to provide essential parameters for modifying the current force field for representing $M^{2+}-\pi$ interaction.

2. Computational Details

The cations used in this study are Li^+, Na^+, K^+, Be^{2+}, Mg^{2+}, and Ca^{2+}. Aromatics selected for investigation are aniline, toluene, phenol, benzene, 1-fluorobenzene, 1,4-difluorobenzene, and 1,3,5-trifluorobenzene. All of the initial structures of the cation−π complexes formed by the above cations and aromatics were designed with the cations located on the normal lines of aromatic rings through the ring centers (Figure 1). They were fully optimized at the B3LYP/6-31G** level followed by the B3LYP/6-311++G(d,p) geometry optimization with an option to disable all of the symmetries. The $R_\perp$ in Figure 1 stands for the interaction distance between a metal cation and an aromatic plane. To estimate the binding enthalpy and free-energy change for the complexation, the frequencies were calculated using B3LYP/6-311++G(d,p) method based on the B3LYP/6-311++G(d,p) geometries. Our previous calculations, as well as others, readily demonstrated that the basis set of 6-311++G-(d,p) is large enough to generally reduce the basis set superposition error (BSSE) to ~1 kcal/mol.[19,22,23] Therefore, the BSSE correction was not taken into account in this study. Morokuma decomposition was carried out at the HF/6-31G** level based on the HF/6-31G** optimized geometry.[24] The Morokuma decomposition results were divided into two parts, electrostatic and nonelectrostatic interactions, to study their contributions to the whole cation−π binding. Although the cation−π interaction between alkaline and substituted benzenes was studied by others with experimental and computational methods,[1,5,12,14,25−28] in this study for the sake of comparison, we included both alkaline metal cations (M^+ hereinafter) and alkaline earth cations (M^{2+} hereinafter).

All of the B3LYP calculations were performed with software Gaussian 98 on a SGI Power Challenge R10000 supercomputer, and all of the Hartree−Fock calculations and Morokuma decompositions were carried out with software G98W and Gamess on Pentium IV PCs.[29,30]

3. Results and Discussion

3.1. Optimized Structures and Atomic Charges. All of the predicted frequencies at the B3LYP/6-311++G(d,p) level were found to have no imaginary values, demonstrating that the optimized structures are true energy minimum structures. Table 1 summarizes the symmetry of the optimized geometries, optimized interaction distance ($R_\perp$), and the calculated Mulliken total atomic charges (Q). The optimized geometries were found to keep the same symmetries as the initial structures. Our B3LYP/6-311++G(d,p) interaction distances are in agreement with the reported B3LYP/6-31G* results with a difference of less than 0.05 Å.[5] The $R_\perp$ shows that the interaction distances between the metal cations (M^{n+}, hereinafter) and the aromatics with electron-withdrawing substituents, π(EWS) hereinafter, are always longer than the distances between the M^{n+} and the aromatics with electron-donating substituents, π(EDS) hereinafter. The Mulliken charges (Q) located on the M^{n+} in the $M^{n+}-\pi$(EDS) complexes are less than those in $M^{n+}-\pi$(EWS). Therefore, the nature of the substituents has impact on the binding distance and charge distribution in a complex. The reason could be that the EDS enrich the electronic density located on the aromatic rings, leading to a stronger electrostatic interaction between the positively charged M^{n+} and the aromatics, resulting in the shorter interaction distances with more charge transfer between the two parts. The Morokuma decomposition results discussed below support this postulation. The positive charges located on the M^{n+}, $Q(M^{n+})$, decrease in the order of $Q(Ca^{2+}) > Q(Mg^{2+}) > Q(Be^{2+})$ and $Q(K^+) > Q(Na^+) > Q(Li^+)$, suggesting that more electrons are transferred from the aromatics to Be^{2+} and to Li^+ for the M^{2+} and M^+, respectively. Therefore, the binding in $Be^{2+}-\pi$ and $Li^+-\pi$ complexes should be stronger than others.

Table 2 lists the Pauling ionic, as well as covalent and van der Waals, radii of the studied metal cations.[31] All of the optimized interaction distances, $R_\perp$, are shorter than the corresponding sum of the van der Waals radius of carbon and the ionic radii of the M^{n+}, $R(C-M^{n+})^b$ in Table 2, except in the $K^+-\pi$(EWS) complexes. This indicates that the interaction between K^+ and π(EWS) is very weak. We found that the optimized interaction distances in the complexes formed by substituted benzenes with Li^+ or M^{2+} are even shorter than the sum of the covalent radii of carbon and corresponding metal elements, $R(C-M^{n+})^c$ in Table 2. This result demonstrates that the interaction between the aromatics and Li^+ or M^{2+} should be rather strong irrespective of substituents attached to benzene.

3.2. Binding Strength. The calculated binding energy (ΔE), binding enthalpy (ΔH), and free-energy change (ΔG) during the complexation reaction, as well as some references' results, were summarized in Table 3.[5,25,26,32,33] The B3LYP/6-311++G-(d,p) predicted results are in good agreement with the experimental results. Generally, the differences are within the experimental error, suggesting again that B3LYP/6-311++G(d,p) is a proper method for studying the cation−π system. However, a systematic difference as large as 2−3 kcal/mol was found between the binding energies calculated at the B3LYP/6-311++G(d,p) and the HF/6-31G** levels for Na^+−aromatic complexes.[33]

The binding strength in the complexes formed by the M^{2+} with all studied aromatics ranges from −54.0 to −254.5 kcal/mol, indicating very strong interactions in comparison with the usual chemical bonding, while the strength in the complexes of the M^+ and aromatics is only −5.5 to −44.3 kcal/mol. These results suggest that the nature of a metal cation is the vital factor affecting its binding strength with aromatics. For example, the binding enthalpy between Be^{2+} and aniline is as strong as −254.5 kcal/mol, while that between Ca^{2+} and aniline is −95.9 kcal/mol. Moreover the binding enthalpy between Li^+ and

TABLE 1: The B3LYP/6-311++G(d,p) Geometrical Parameter and Mulliken Charge

		Li^+		Na^+		K^+		Be^{2+}		Mg^{2+}		Ca^{2+}	
X	symmetry	$R_\perp$, Å	Q, e	$R_\perp$, Å	Q, e	$R_\perp$, Å	Q, e	$R_\perp$, Å	Q, e	$R_\perp$, Å	Q, e	$R_\perp$, Å	Q, e
$-NH_2$	C_s	1.821	0.442	2.383	0.757	2.841	0.965	1.281	0.578	1.835	0.924	2.334	1.442
$-CH_3$	C_s	1.822	0.388	2.386	0.723	2.863	0.927	1.275	0.583	1.924	0.882	2.349	1.400
$-OH$	C_1	1.845	0.459	2.410	0.774	2.891	0.967	1.293	0.590	1.937	0.978	2.363	1.480
$-H$	C_{6v}	1.842	0.452	2.408	0.767	2.904	0.946	1.290	0.645	1.941	1.017	2.371	1.469
$-F$	C_s	1.875	0.483	2.441	0.789	2.939	0.970	1.303	0.607	1.965	1.031	2.388	1.507
1,4-2F	C_{2v}	1.902	0.516	2.489	0.820	2.996	0.990	1.318	0.572	1.976	1.048	2.405	1.542
1,3,5-3F	C_{3v}	1.982	0.579	2.538	0.854	3.058	1.009	1.366	0.514	2.024	1.036	2.434	1.610

TABLE 2: The Ionic, Covalent, and van der Waals Radii and the Optimized Interaction Distance (Å)

	Li^+	Na^+	K^+	Be^{2+}	Mg^{2+}	Ca^{2+}
Pauling ionic radius	0.60	0.95	1.33	0.31	0.65	0.99
covalent radius (M)[a]	1.34	1.54	1.96	0.90	1.30	1.74
$R(C-M^{n+})$[b]	2.30	2.65	3.03	2.01	2.35	2.69
$R(C-M^{n+})$[c]	2.11	2.31	2.73	1.67	2.07	2.51
$R_\perp$[d]	1.82−1.98	2.38−2.54	2.84−3.06	1.28−1.37	1.84−2.02	2.33−2.43

[a] Empirical covalent radius.[31] [b] The sum of the van der Waals radius of C (1.70 Å) and the Pauling ionic radii of the metal cations. [c] The sum of the covalent radius of C (0.77 Å) and that of the metal atoms. [d] The optimized interaction distance between substituted benzene and metal cation.

TABLE 3: The Calculated Thermodynamic Parameters (kcal/mol) at B3LYP/6-311++G(d,p) Level

A. Complexes Formed by Alkaline Metal Cations and Substituted Benzenes

	Li^+				Na^+				K^+			
X	ΔE	ΔH	ΔG	ΔH	ΔE	ΔH	ΔG	ΔH	ΔE	ΔH	ΔG	ΔH
$-NH_2$	−45.44	−44.32	−36.15		−29.52	−28.82	−21.35	−31.8[d]	−21.20	−20.59	−13.49	
$-CH_3$	−41.38	−40.26	−31.47	−44.6[a]	−25.93	−25.29	−17.23	−27.2[a]	−17.71	−17.24	−9.62	−19.3[a]
$-OH$	−39.07	−37.92	−29.68		−24.37	−23.65	−16.24	−23.5[b] −26.9[d]	−16.69	−16.13	−9.16	
$-H$	−38.43	−37.33	−29.67	−37.9[c]	−23.90	−23.26	−16.37	−21.2b −27.1[d]	−16.24	−15.60	−10.44	−18.3[c]
$-F$	−32.54	−31.48	−23.46		−19.31	−18.66	−11.46	−22.0[d]	−12.56	−12.08	−5.38	
1,4-2F	−26.52	−25.64	−17.70		−14.65	−14.14	−7.17	−16.8[d]	−8.95	−8.57	−2.11	
1,3,5-3F	−21.15	−20.39	−13.76		−10.67	−10.21	−4.53	−12.4[d]	−5.88	−5.49	+0.33	

B. Complexes Formed by Alkaline Earth Metal Cations and Substituted Benzenes

	Be^{2+}				Mg^{2+}				Ca^{2+}			
X	ΔE	ΔH	ΔG	ΔH	ΔE	ΔH	ΔG	ΔH	ΔE	ΔH	ΔG	ΔH
$-NH_2$	−256.34	−254.53	−245.27		−138.22	−137.30	−128.54		−96.79	−95.87	−87.45	
$-CH_3$	−241.88	−240.69	−230.88		−126.83	−126.28	−116.88		−86.87	−86.34	−77.37	
$-OH$	−236.54	−235.03	−225.81		−122.81	−122.03	−113.32		−83.84	−83.05	−74.68	
$-H$	−229.47	−228.15	−220.64	−237.5[e]	−118.11	−117.45	−110.45	−124.1[e]	−79.93	−79.30	−71.54	−72.3[e]
$-F$	−216.54	−215.19	−206.20		−107.60	−106.93	−98.49		−71.15	−70.51	−62.37	
1,4-2F	−203.17	−201.94	−192.54		−96.56	−96.05	−87.25		−62.07	−61.63	−53.14	
1,3,5-3F	−190.97	−189.76	−181.89		−87.34	−86.85	−79.61		−54.54	−53.98	−46.41	

[a] Experimental result.[25] [b] Experimental result.[26] [c] Experimental result.[32] [d] HF/6-31G** result.[33] [e] B3LYP/6-31G* result.[5]

aniline is −44.32 kcal/mol, whereas that between K^+ and aniline is only −20.59 kcal/mol. Regarding the same metal cation, M^{n+}, the binding in the $M^{n+}-\pi$(EDS) complexes is stronger than that in M^{n+}−benzene complexes, while that in the $M^{n+}-\pi$(EWS) complexes is the weakest. This demonstrates that the existence of EWS in an aromatic system weakens the binding of the aromatic with M^{n+}, while the EDS enhances the binding.

As the substituents become more and more electron-withdrawing, the binding strength becomes weaker and weaker (Table 3), suggesting a correlation between the electronic properties of a substituent and the binding strength. Table 4 lists the Hammett electronic parameters (σ) of these studied substituents, which are the electronic effect of a substituent relative to hydrogen.[34,35] The σ values in Table 4 include the parameters of the substituents at the para and meta positions, σ_{meta} and σ_{para}, respectively. The values suggest that as the σ values increase, the binding strength weakens. The best correlation was found through the regression analysis between the calculated binding enthalpies and the total Hammett electronic parameter, σ_{total} ($\sigma_{total} = \sigma_{meta} + \sigma_{para}$), rather than σ_{meta} or σ_{para}. The correlation coefficients, R^2, range from 0.98 to 0.99 (Figure 2), demonstrating that the total electronic effect of the substituents, including induction and resonance, vitally impacts the total binding strength. This might be caused by the unusual interaction pattern in the cation$-\pi$ complexes, in which the M^{n+} interacts with all aromatic ring atoms. Therefore, both para and meta positions, that is, σ_{meta} and σ_{para}, should have an effect on the final total binding energy.

TABLE 4: The Hammett Electronic Parameters

X	σ_{meta}[34,35]	σ_{para}[34,35]	σ_{total}
$-NH_2$	−0.16	−0.66	−0.82
$-CH_3$	−0.07	−0.17	−0.24
$-OH$	0.12	−0.37	−0.25
$-H$	0.0	0.0	0.0
$-F$	0.34	0.06	0.40
1,4-2F	0.68	0.12	0.80
1,3,5-3F	1.04	0.18	1.22

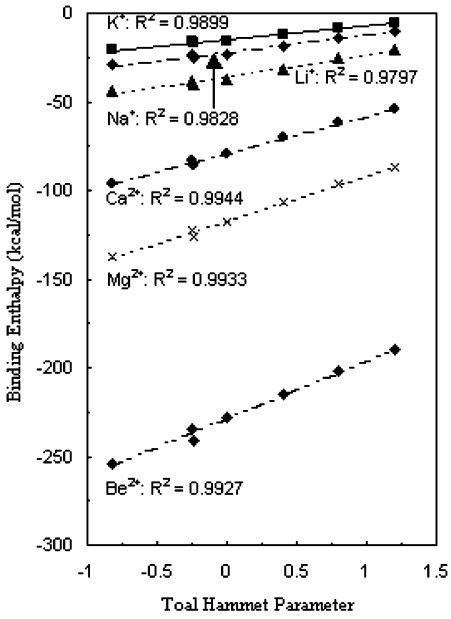

Figure 2. The correlation between σ_{total} and binding enthalpy.

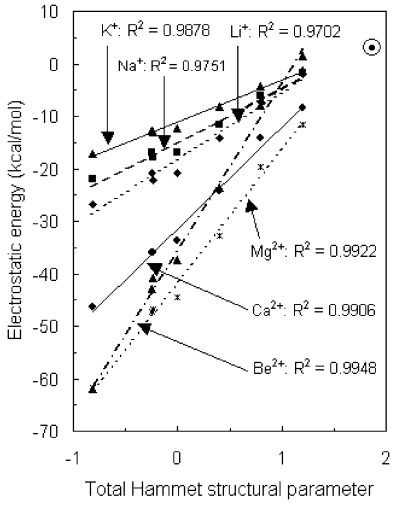

Figure 3. The correlation between σ_{total} and electrostatic energy.

3.3. Electrostatic and Nonelectrostatic Contributions. Table 5 summarizes the Morokuma decomposition results on the binding energy calculated by the software Gamess at the HF/6-31G(d,p) level.[29] The binding energy is divided into two parts, electrostatic and nonelectrostatic, to explore the distributions of the electrostatic and nonelectrostatic onto the cation−π binding. The nonelectrostatic is calculated as the difference between the total binding energy and the electrostatic force. In comparison with the result of Cubero and coworkers of the electrostatic contribution to the total binding strength for the complexes formed by Na^+ with substituted benzenes, a slight difference, ~2 kcal/mol, was found between their result and ours, demonstrating that the Morokuma decomposition result is reliable.[33] Similar to the conclusion, drawn from the complexes formed by Na^+ with the substituted benzenes, that the nonelectrostatic component is a constant to the total binding energy,[36] the data in Table 5 demonstrate that nonelectrostatic contribution to the whole binding energies of a M^{n+} with different substituted benzenes is only affected by the nature of the metal cation. Generally, the substituents have no impact on the nonelectrostatic contribution. However, the electrostatic contribution is affected by the nature of both the M^{n+} and substituents. For instance, the electrostatic component is −17.13 kcal/mol in the K^+−aniline complex, −61.91 kcal/mol in the Be^{2+}−aniline complex, and +1.55 kcal/mol in the complex formed by Be^{2+} and 1,3,5-trifluorobenzene.

The proportion of the electrostatic to the total binding energy in the complexes formed by the M^+ with the aromatics is significantly larger than that in the complexes formed by the M^{2+} and the aromatics, suggesting that electrostatic component is much more important to the binding of M^+ with aromatics than to that of M^{2+}. This is specially so in the M^+−π(EDS) complexes because the proportions are always higher than 50%. In the case of the K^+−aniline complex, the proportion is as high as 82%, demonstrating that the binding is electrostatic in nature. However, the proportion in the complexes formed by the M^{2+} and all of the aromatics is less than 50% except in some Ca^{2+}−π(EDS) complexes, demonstrating that the non-

TABLE 5: The Morokuma Decomposition on Binding Energy (kcal/mol) at HF/6-31G(d,p) Level[a]

A. Complexes Formed by Alkaline Metal Cations and Substituted Benzenes

	Li^+				Na^+				K^+			
X	ΔE	E_{el}	$E_{el}/\Delta E$	E_{nel}	ΔE	E_{el}	$E_{el}/\Delta E$	E_{nel}	ΔE	E_{el}	$E_{el}/\Delta E$	E_{nel}
$-NH_2$	−45.77	−26.85	58.66	−18.92	−30.77	−21.96	71.37	−8.81	−20.81	−17.13	82.32	−3.68
$-CH_3$	−41.52	−22.10	53.23	−19.42	−27.18	−17.81	65.53	−9.37	−17.17	−12.94	75.36	−4.23
−OH	−39.52	−20.72	52.43	−18.80	−25.94	−16.91	65.19	−9.03	−16.68	−12.74	76.38	−3.94
−H	−39.06	−20.83	53.33	−18.23	−25.65	−16.85	65.69	−8.80	−16.20	−12.29	75.86	−3.91
−F	−32.84	−14.23	43.33	−18.61	−20.72	−11.50	55.50	−9.22	−12.36	−8.22	66.50	−4.14
1,4-2F	−26.29	−7.20	27.39	−19.09	−15.62	−5.98	38.28	−9.64	−8.49	−4.19	49.35	−4.30
1,3,5-3F	−20.96	−1.86	8.87	−19.10	−11.60	−1.82	15.69	−9.78	−5.52	−1.17	21.20	−4.35

B. Complexes Formed by Alkaline Earth Metal Cations and Substituted Benzenes

	Be^{2+}				Mg^{2+}				Ca^{2+}			
X	ΔE	E_{el}	$E_{el}/\Delta E$	E_{nel}	ΔE	E_{el}	$E_{el}/\Delta E$	E_{nel}	ΔE	E_{el}	$E_{el}/\Delta E$	E_{nel}
$-NH_2$	−264.79	−61.91	23.38	−202.88	−140.64	−61.61	43.81	−79.03	−82.52	−46.26	56.06	−36.26
$-CH_3$	−242.42	−40.89	16.87	−201.53	−124.59	−46.77	37.54	−77.82	−72.99	−35.93	49.23	−37.06
−OH	−241.28	−42.76	17.72	−198.52	−123.75	−47.26	38.19	−76.49	−71.43	−35.95	50.32	−35.48
−H	−231.31	−37.34	16.14	−193.97	−118.03	−44.38	37.60	−73.65	−68.14	−33.70	49.46	−34.44
−F	−219.53	−23.54	10.72	−195.99	−110.01	−32.73	29.75	−77.28	−59.28	−24.32	41.03	−34.96
1,4-2F	−207.04	−7.98	3.85	−199.06	−96.76	−19.60	20.26	−77.16	−49.61	−14.09	38.48	−35.52
1,3,5-3F	−197.42	+1.55	−0.79	−198.97	−89.21	−11.63	13.37	−77.58	−43.86	−8.30	18.92	−35.56

[a] ΔE = binding energy corrected by BSSE; E_{el} = electrostatic contribution; $E_{el}/\Delta E$ = the percentage of electrostatic contribution in whole binding energy; E_{nel} = nonelectrostatic contribution.

TABLE 6: The Bonding Molecular Orbital Composition Analysis Result at B3LYP/6-31G Level**

A. Complexes Formed by Substituted Benzenes and Be^{2+}

X	MO no.	energy, eV	MO comp (%)				contrib from C (%)				contrib from Be^{2+} (%)				contrib from X (%)			
			C	H	X	Be^{2+}	s	p_x	p_y	p_z	s	p_x	p_y	p_z	s	p_x	p_y	p_z
1,3,5-3F	34	−19.5777	57.54	0.03	28.61	13.83	1.54	0.85	0.66	53.98	0.00	13.55	0.02	0.00	0.19	0.27	0.19	27.94
	33	−19.5782	57.53	0.03	28.61	13.83	1.54	0.66	0.85	53.97	0.00	0.02	13.55	0.00	0.19	0.19	0.27	27.94
	31	−21.5064	28.13	0.02	60.39	11.46	6.47	1.44	1.44	18.36	9.84	0.00	0.00	1.62	0.75	0.01	0.01	59.53
1,4-2F	30	−19.0250	50.00	0.01	36.39	13.59	2.22	0.07	1.67	45.55	0.00	0.00	13.36	0.00	0.34	0.00	0.13	35.90
	29	−20.3513	84.10	0.11	0.54	15.25	1.99	0.60	1.60	79.39	0.00	15.00	0.00	0.00	0.00	0.54	0.00	0.00
	26	−21.7432	27.90	0.12	61.47	10.51	0.99	0.07	2.17	24.27	9.23	0.00	0.00	1.26	0.26	0.00	0.12	61.00
−F	26	−19.3885	60.52	0.09	25.47	13.92	2.22	1.68	0.37	55.89	0.46	13.22	0.00	0.03	0.21	0.01	0.00	25.23
	25	−20.0988	84.66	0.73	0.08	14.54	2.09	2.00	2.78	77.43	0.00	0.00	14.31	0.00	0.00	0.00	0.08	0.00
	21	−22.3230	48.37	0.33	38.60	12.70	2.17	2.13	1.36	42.40	10.83	0.43	0.00	1.39	0.13	0.32	0.00	38.09
−OH	26	−18.2065	48.23	0.05	39.25	12.42	1.73	2.56	0.18	43.39	0.90	11.32	0.02	0.03	0.24	0.14	0.01	38.81
	25	−19.5953	83.85	1.85	0.74	13.49	1.85	2.98	6.59	72.11	0.00	0.01	13.28	0.00	0.16	0.06	0.49	0.03
	19	−23.0545	67.88	3.99	18.03	10.05	5.15	3.92	8.18	50.43	8.35	0.54	0.21	0.87	0.12	0.06	0.01	17.77
$-CH_3$	26	−18.5531	50.71	0.08	37.64	11.56	1.14	2.00	0.61	46.67	0.76	10.66	0.00	0.01	0.17	0.14	0.00	21.13
	24	−19.4979	82.97	0.59	2.13	14.32	2.45	2.72	1.76	75.72	0.00	0.00	14.13	0.00	0.00	0.00	1.45	0.00
	19	−22.5813	75.80	0.65	5.07	18.48	3.01	3.09	1.70	67.73	16.46	0.21	0.00	1.71	0.13	0.43	0.00	3.09
$-NH_2$	26	−17.0769	42.84	0.06	44.98	12.02	1.29	3.57	0.19	37.52	1.65	10.11	0.00	0.13	0.16	0.45	0.00	44.26
	25	−19.0748	83.97	3.03	0.11	12.89	1.73	3.31	10.33	68.28	0.00	0.00	12.70	0.00	0.00	0.00	0.03	0.00
	21	−22.2422	76.04	2.53	7.65	13.79	5.32	5.26	4.08	61.14	12.18	0.22	0.00	1.33	0.32	0.15	0.00	7.11

B. Complexes Formed by Substituted Benzenes and K^+

X	MO no.	energy, eV	MO comp (%)				contrib from C (%)				contrib from K^+ (%)				contrib from X (%)			
			C	H	X	K^+	s	p_x	p_y	p_z	s	p_x	p_y	p_z	s	p_x	p_y	p_z
1,3,5-3F	40	−13.6997	47.55	0.23	50.90	1.32	6.28	1.55	1.55	37.91	0.45	0.00	0.00	0.51	0.39	0.01	0.01	50.45
	32	−17.3147	33.93	0.02	63.81	2.24	0.13	0.08	0.08	33.59	0.75	0.00	0.00	1.39	0.01	0.00	0.00	63.67
1,4-2F	37	−11.7228	98.13	0.14	0.00	1.83	0.67	0.14	96.88	0.18	0.00	0.00	0.00	1.54	0.00	0.00	0.00	0.00
	35	−13.8346	49.78	0.01	48.27	1.93	0.16	0.15	49.20	0.02	0.67	0.00	0.87	0.00	0.07	0.06	48.11	0.00
	28	−16.7863	30.36	0.01	67.49	2.14	0.09	0.01	30.15	0.04	0.75	0.00	1.29	0.00	0.02	0.01	67.35	0.00
−F	34	−10.9698	80.69	0.04	17.74	1.53	0.80	50.47	29.03	0.07	0.02	0.17	0.87	0.00	0.07	11.56	6.10	0.00
	33	−11.4553	97.92	0.05	0.00	2.03	0.62	61.25	35.56	0.19	0.00	0.00	0.00	1.72	0.00	0.00	0.00	0.00
	31	−14.0583	69.39	0.27	26.69	3.65	0.36	43.27	25.33	0.14	1.31	0.76	1.17	0.00	0.05	18.69	7.92	0.00
−OH	33	−11.1902	97.65	0.05	0.04	2.25	0.62	50.35	45.80	0.59	0.01	0.00	0.00	1.90	0.00	0.02	0.02	0.00
	31	−13.3285	58.36	9.60	30.10	1.94	0.31	19.60	16.25	21.90	0.71	0.16	0.85	0.00	1.59	8.41	18.97	0.41
	28	−15.2382	51.40	0.69	45.14	2.77	0.84	31.73	17.52	1.21	0.92	1.30	0.37	0.00	1.39	12.61	30.66	0.06
$-CH_3$	34	−10.7244	87.11	0.03	10.74	2.13	0.68	35.08	50.96	0.10	0.00	0.86	0.81	0.00	0.02	1.39	2.51	0.00
	33	−11.0474	97.38	0.05	0.16	2.41	0.45	40.35	56.16	0.15	0.00	0.00	0.00	2.06	0.00	0.00	0.00	0.09
	30	−13.6561	64.39	0.06	31.02	4.53	0.18	27.23	36.69	0.06	1.76	0.61	1.75	0.00	0.01	5.91	11.59	0.00
$-NH_2$	33	−10.9587	97.47	0.05	0.08	2.40	0.72	40.43	55.67	0.37	0.00	0.00	0.00	2.05	0.00	0.00	0.00	0.04
	32	−12.4488	55.36	0.30	42.26	2.09	0.40	25.28	29.29	0.14	0.48	0.10	1.20	0.00	2.37	9.00	30.65	0.00
	29	−14.4722	75.60	1.21	18.10	5.06	1.07	39.87	34.03	0.50	1.81	1.65	1.22	0.00	0.90	2.79	14.33	0.00

C. Complexes Formed by Benzene and M^{n+}

M^{n+}	MO no.	energy, eV	MO comp (%)			contrib from C (%)				contrib from M^{n+} (%)			
			C	H	M^{n+}	s	p_x	p_y	p_z	s	p_x	p_y	p_z
Be^{2+}	22	−19.8890	84.92	0.25	14.83	2.71	1.36	1.41	79.10	0.00	0.23	14.39	0.00
	21	−19.8895	84.92	0.25	14.83	2.71	1.41	1.36	79.10	0.00	14.39	0.23	0.00
	18	−22.8879	78.92	0.33	20.75	3.13	1.55	1.55	72.36	18.56	0.00	0.00	2.10
Mg^{2+}	26	−18.0299	89.44	0.08	10.48	1.02	0.65	0.69	86.72	0.00	0.32	8.96	0.00
	25	−18.0307	89.44	0.08	10.49	1.02	0.68	0.65	86.72	0.00	8.96	0.32	0.00
	22	−21.3595	67.63	0.17	32.30	1.64	1.17	1.17	63.28	25.19	0.00	0.00	6.43
Ca^{2+}	30	−16.6619	94.88	0.05	5.08	1.20	0.53	0.66	92.17	0.00	0.00	3.19	0.00
	29	−16.6619	94.88	0.05	5.08	1.20	0.66	0.53	92.17	0.00	3.19	0.00	0.00
	26	−19.7428	86.78	0.09	13.13	0.64	0.43	0.43	84.97	6.83	0.00	0.00	4.10
Li^+	22	−12.5367	93.87	0.15	5.98	0.47	0.17	0.30	92.64	0.00	0.00	5.80	0.00
	21	−12.5367	93.87	0.15	5.98	0.47	0.30	0.17	92.64	0.00	5.80	0.00	0.00
	18	−15.6105	82.90	0.03	17.07	1.42	0.24	0.24	80.75	9.55	0.00	0.00	7.28
Na^+	26	−11.7687	97.91	0.04	2.05	0.20	0.12	0.16	97.17	0.00	0.00	1.84	0.00
	25	−11.7687	97.91	0.04	2.05	0.20	0.16	0.12	97.17	0.00	1.84	0.00	0.00
	22	−14.8986	89.75	0.03	10.22	0.56	0.14	0.14	88.69	6.24	0.00	0.00	3.63
K^+	30	−11.1695	97.74	0.04	2.22	0.55	96.66	0.11	0.17	0.00	0.00	0.11	1.78
	29	−11.1706	97.74	0.04	2.22	0.56	96.66	0.16	0.12	0.00	0.00	1.78	0.11
	26	−14.2328	93.36	0.06	6.58	0.12	92.92	0.07	0.08	2.52	3.51	0.00	0.00

electrostatic contribution dominates the bindings of the Be^{2+} or Mg^{2+} with aromatics.

The electrostatic contribution to the total binding energy decreases as the Hammett electronic parameter increases (Tables 4 and 5). This is because the total binding energy is correlated with Hammett electronic parameters, while the nonelectrostatic contribution remains almost a constant. Figure 3 depicts the relationship between the electrostatic energy and σ_{total}. The R^2 shown in Figure 3, ranging from 0.97 to 0.99, demonstrates that the correlation is very strong. Furthermore, the extension lines roughly intersect each other at the circled dot (top right in Figure 3), where as the electrostatic contribution is +2.5 kcal/

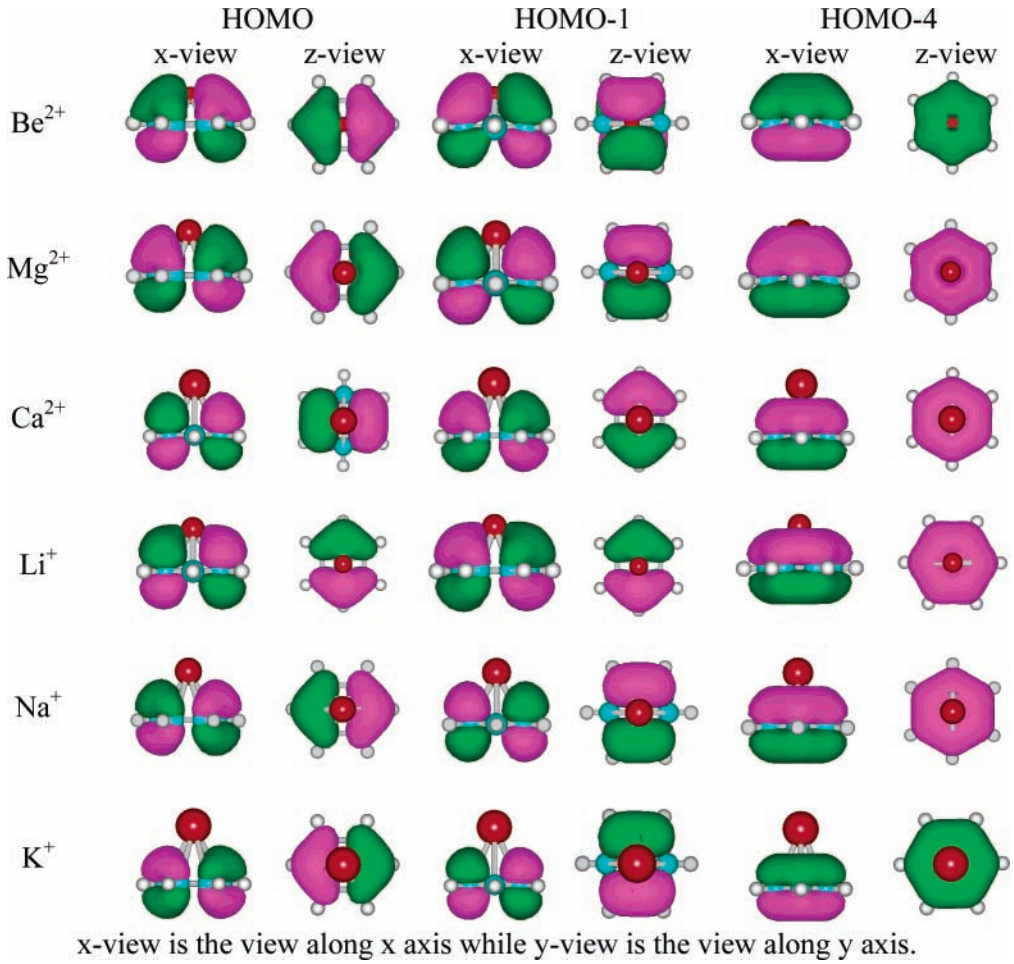

Figure 4. The bonding MO features of M^{n+}−benzene complexes.

mol and total Hammett electronic parameter is 1.8, except the line belonging to Be^{2+}. The exception of Be^{2+} might result from its unusual geometry, in which the hydrogen atoms of the aromatics make an out-of-plane shift toward Be^{2+}, leading to significant electrostatic repulsion between positively charged hydrogen atoms and Be^{2+}, resulting in a very steep slope. At the intersection point, the binding strength is totally contributed by nonelectrostatic components.

3.4. Orbital Interaction. The molecular orbital (MO) component analysis was carried out for the first 10 occupied MOs of the complexes formed by Be^{2+} with the substituted benzenes and of the complexes formed by K^+ with the aromatics to explore whether and how the atomic orbital of a metal cation interacts with the orbital of aromatics. While the former stands for the strong nonelectrostatic interaction complex, that of the later is strongly electrostatic. The MO analysis results are summarized in Table 6.

Each complex formed by Be^{2+} with substituted benzenes has three bonding MOs that are contributed jointly by both the aromatics and the metal cation, which are the highest occupied molecular orbital (HOMO), HOMO-1, and HOMO-4 (Table 6, section A). The orbital contribution of Be^{2+} to the HOMO, HOMO-1, and HOMO-4 in different Be^{2+}−aromatic complexes is 12−14%, 13−15%, and 10−18%, respectively. Those hydrogen atoms attached to the aromatic ring have no obvious contribution to the bonding MOs, therefore, playing no contribution to the cation−π bindings. Further analysis on the atomic orbital shows that only the p_z orbital of the aromatic carbon atoms is obviously involved in the three bonding MOs (Table 6, section A), suggesting that it is the π orbital of the aromatics that interacts with metal cation. However, it is the s, p_x, or p_y orbital of Be^{2+}, rather than the p_z orbital, that has obvious contribution to the bonding MOs, demonstrating that the p_z orbital of Be^{2+}, which orientates toward the center of the benzene ring, is not important for the binding between Be^{2+} and aromatics. Therefore, we can infer from these observations that the orbital interaction characteristic between Be^{2+} and aromatics is largely the s−π, p_x−π, and p_y−π interactions.

Table 6, section B, shows that the contribution from all atomic orbitals of K^+ to any bonding MO is very little, less than 5%, suggesting that the orbital interactions between K^+ and aromatics are not important. Therefore, the nonelectrostatic interaction between K^+ and aromatics is very week. This conjecture is totally in agreement with the conclusion drawn from the above Morokuma analysis with results strongly indicating that the electrostatic contribution is the dominant component in the binding of K^+ to aromatics.

Sections A and B of Table 6 also indicate that the contribution of the atomic orbital from a metal cation to the bonding MOs is largely unchanged as the substituent varies from the electron-withdrawing to the electron-donating type. This is in agreement with the conclusion based on the Morokuma decomposition that the nonelectronic interaction is a constant in the complexes formed by different substituted benzenes with the same cation.

Because the orbital interaction between different aromatics and the same metal cation is largely unaffected by the substituents, only the complexes formed by benzene and different M^{n+} were selected to carry out further molecular orbital composition analysis to further explore the characteristics of their orbital interaction. The analyzed results were shown in Table 6, section

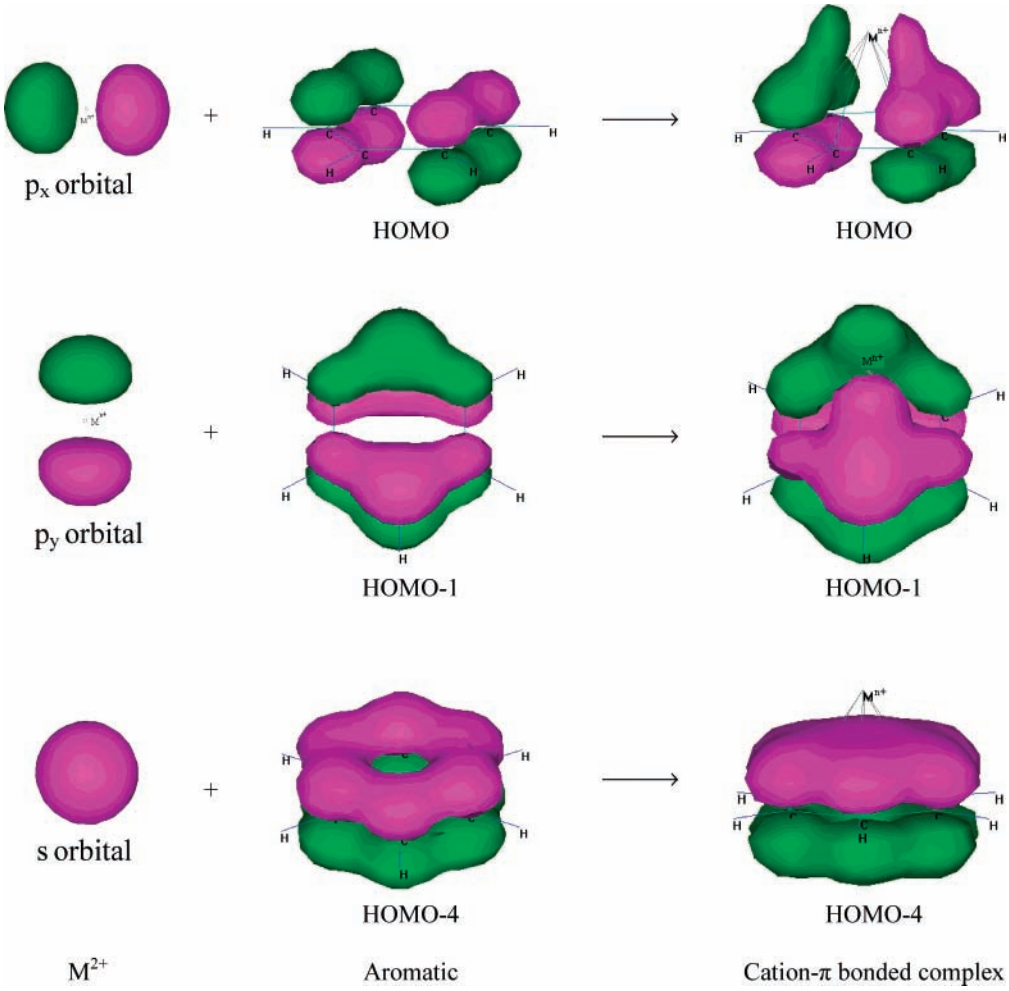

Figure 5. The orbital interaction between aromatics and Be^{2+} or Mg^{2+} for forming cation$-\pi$ bond.

C. It is clear that the atomic orbital contribution from the metal cations to the bonding MOs decreases as the cation changes in the order of Be^{2+}, Mg^{2+}, Ca^{2+}, Li^{+}, Na^{+}, and K^{+}. The strong orbital interaction was found in $Be^{2+}-$benzene and $Mg^{2+}-$benzene complexes. We also observed that more than 10% of each of the three bonding MOs is from either of these two metal cations. However, the orbital interaction in the complexes formed by the rest of the cations is comparatively weak. Figure 4 depicts all of the MO features listed in Table 6, section C, with the orbital contour value of 0.025 e $Å^{-3}$.[37] The bonding MO features demonstrate again the very strong orbital interaction of benzene with Be^{2+} and Mg^{2+}. In summary, the orbital interaction between the M^{2+} and an aromatic to form a cation$-\pi$ bond can be illustrated as in Figure 5. In details, the p_x orbital of a metal cation interacts with the HOMO of the aromatic to form the HOMO of the cation$-\pi$ bonded complex; the p_y orbital of the metal cation interacts with the HOMO-1 of the aromatic to form the HOMO-1 of their complex; and the s orbital of the metal interacts with the HOMO-4 of the aromatic to form the complex's HOMO-4.

4. Conclusions

The B3LYP/6-311++G** optimized geometries, the interaction distances, the calculated binding strength, the binding energy component analysis results, the molecular orbital decomposition, and the molecular orbital contour feature demonstrate that the interaction between substituted benzenes and Be^{2+} or Mg^{2+} is in nature a chemical bonding that we like to name cation$-\pi$ bond. The interaction distances between the cations and the aromatic rings are even shorter than the covalent bond length between carbon and corresponding metal. The total binding strength is always stronger than -89 kcal/mol no matter which substituted benzenes are involved. The proportion of electrostatic contribution to their whole binding energy is always less than 50%. The nonelectrostatic interaction is always stronger than -73 kcal/mol, which is significantly stronger than the chemical bonding between two fluorine atoms (-33 kcal/mol). The nonelectrostatic interaction is almost unaffected by the nature of the substituents attached to the benzene ring, while strong correlations were found between the total binding enthalpy and the Hammett electronic parameters of the substituents and between the electrostatic and the Hammett parameters. The binding is pure nonelectrostatic if the total Hammet electronic parameter is as large as 1.8. The molecular orbital composition analysis and the orbital contour map suggest a strong orbital interaction between the s, p_x, and p_y orbitals of these metal cations and the π orbital of the aromatic. In conclusion, the characteristics of a cation$-\pi$ bond can be summarized as short interaction distance, strong binding strength, significant nonelectrostatic interaction, dominant proportion of nonelectrostatic interaction in the whole binding strength, constant nonelectrostatic interaction between the same metal cation and different aromatics, and strong orbital interaction between the s, p_x, and p_y orbitals of the metal cation and the π orbital of the aromatics. Therefore, a cation$-\pi$ bond could be quite easily identified on the basis of the geometrical, thermo-

chemical, and orbital parameters described above. All of these results are helpful for us in understanding cation−π bonding. It is also useful in improving the existing force field for reproducing such an unusual bonding that is heavily involved in many systems, especially in many biological processes.

Acknowledgment. We acknowledge the financial supports from the National Natural Science Foundation of China (Grant 2002CB512802) and the State Key Program of Basic Research of China (Grant 1998051115). The quantum chemistry calculations were performed on Power Challenge R10000 at the Network Information Center, Chinese Academy of Sciences, Beijing, P. R. China, and on P4 PCs at Singapore Polytechnic, Singapore.

References and Notes

(1) Ma, J. C.; Doughterty, D. A. *Chem Rev.* **1997**, *97*, 1303.
(2) Ward, S. D.; Curtis, C. A.; Hulme, E. C. *Mol. Pharmacol*. **1999**, *56*, 1031.
(3) Carlier, P. R.; Chow, E. S.; Han, Y.; Liu, J.; Yazal, J. E.; Pang, Y. P. *J. Med. Chem*. **1999**, *42*, 4225.
(4) Cabarcos, O.; Weinheimer, C.; Lisy, J. *J. Chem. Phys*. **1999**, *110*, 8429.
(5) Choi, H. S.; Suh, S. B.; Cho, S. J.; Kim, K. S. *Proc. Natl. Acad. Sci. U.S.A*. **1998**, *95*, 12094.
(6) Roelens, S.; Torriti, R. *J. Am. Chem. Soc*. **1998**, *120*, 12443.
(7) Gallivan, J. P.; Dougherty, D. A. *Proc. Natl. Acad. Sci. U.S.A*. **1999**, *96*, 9459.
(8) Macias, A.; Rajamani, R.; Evanseck, J. *Abst. Pap. Am. Chem. Soc*. **1997**, *214*, 105.
(9) Minoux, H.; Chipot, C. *J. Am. Chem. Soc.* **1999**, *121*, 10366.
(10) Wintjens, R.; Lievin, J.; Rooman, M.; Buisine, E. *J. Mol. Biol.* **2000**, *302*, 395.
(11) McFail-Isom, L.; Shui, X.; Williams, L. D. *Biochemistry* **1998**, *37*, 17105.
(12) Kim, K. S.; Tarakeshwar, P.; Lee, J. Y. *Chem. Rev*. **2000**, *100*, 4145.
(13) Wouters, J. *Protein Sci.* **1998**, *7*, 2472.
(14) Nicklaus, M. C.; Neamati, N.; Hong, H.; Mazumder, A.; Sunder, S.; Chen, J.; Milne, G. W.; Pommier, Y. *J. Med. Chem*. **1997**, *40*, 920.
(15) Zarić, S.; Popvić, D. M.; Knapp, E.-W. *Chem.—Eur. J*. **2000**, *6*, 3935.
(16) Zacharias, N.; Dougherty, D. A. *Trends Pharmacol. Sci*. **2002**, *23*, 281.
(17) Mo, Y.; Subramanian, G.; Gao, J.; Ferguson, D. M. *J. Am. Chem. Soc.* **2002**, *124*, 4832.
(18) Shi, Z.; Olson, A.; Kallenbach, N. R. *J. Am. Chem. Soc*. **2002**, *124*, 3284.
(19) Zhu, W. L.; Tan, X. J.; Puah, C. M.; Gu, J. D.; Jiang, H. L.; Chen, K. X.; Felder, C. E.; Silman, I.; Sussman, J. L. *J. Phys. Chem. A* **2000**, *104*, 9573.
(20) Williams, K.; Pahk, A. J.; Kashiwagi, K.; Masuko, T.; Nguyen, N. D.; Igarashi, K. *Mol. Pharmacol.* **1998**, *53*, 933.
(21) Tan, X.-J.; Zhu, W.-L.; Cui, M.; Luo, X.-M.; Gu, J.-D.; Silman, I.; Sussman, J. L.; Jiang, H.-L.; Ji, R.-Y.; Chen, K.-X. *Chem. Phys. Lett*. **2001**, *349*, 113.
(22) Peschke, M.; Blades, A. T.; Kebarle, P. *J. Am. Chem. Soc*. **2000**, *122*, 10440.
(23) Zhu, W.-L.; Puah, C. M.; Tan, X. J.; Hiang, H. L.; Chen, K. X. *J. Phys. Chem. A* **2001**, *105*, 426.
(24) Kitaura, K.; Morokuma, K. *Int. J. Quantum Chem.* **1976**, *10*, 325−340
(25) Amunugama, R.; Rodgers M. T. *J. Phys. Chem. A* **2002**, *106*, 5529.
(26) Amunugama, R.; Rodgers M. T. *J. Phys. Chem. A* **2000**, *104*, 2238.
(27) Tsuzuki, S.; Yoshida, M.; Uchimaru, T.; Mikami, M. *J. Phys. Chem. A* **2001**, *105*, 769.
(28) Liu, T.; Gu, J. D.; Tan, X. J.; Zhu, W.-L.; Luo, X.-M.; Jiang, H. L.; Ji, R.-Y.; Chen, K. X.; Silman, I.; Sussman, J. L. *J. Phys. Chem. A* **2001**, *105*, 5431.
(29) Schmidt, M. W.; Baldridge, K. K.; Boatz, J. A.; Elbert, S. T.; Gordon, M. S.; Jensen, J. H.; Koseki, S.; Matsunaga, N. *J. Comput. Chem.* **1993**, *14*, 1347.
(30) Frisch, M. J.; Trucks, G. W.; Schlegel, H. B.; Scuseria, G. E.; Robb, M. A.; Cheeseman, J. R.; Zakrzewski, V. G.; Montgomery, J. A., Jr.; Stratmann, R. E.; Burant, J. C.; Dapprich, S.; Millam, J. M.; Daniels, A. D.; Kudin, K. N.; Strain, M. C.; Farkas, O.; Tomasi, J.; Barone, V.; Cossi, M.; Cammi, R.; Mennucci, B.; Pomelli, C.; Adamo, C.; Clifford, S.; Ochterski, J.; Petersson, G. A.; Ayala, P. Y.; Cui, Q.; Morokuma, K.; Malick, D. K.; Rabuck, A. D.; Raghavachari, K.; Foresman, J. B.; Cioslowski, J.; Ortiz, J. V.; Stefanov, B. B.; Liu, G.; Liashenko, A.; Piskorz, P.; Komaromi, I.; Gomperts, R.; Martin, R. L.; Fox, D. J.; Keith, T.; Al-Laham, M. A.; Peng, C. Y.; Nanayakkara, A.; Gonzalez, C.; Challacombe, M.; Gill, P. M. W.; Johnson, B. G.; Chen, W.; Wong, M. W.; Andres, J. L.; Head-Gordon, M.; Replogle, E. S.; Pople, J. A. *Gaussian 98*, revision D.7; Gaussian, Inc.: Pittsburgh, PA, 1998.
(31) Winter, M. Webelements Periodic Table (professional edition). http://www.webelements.com/webelements/ (accessed Aug 2002), University of Sheffield, Sheffield, England.
(32) (a) Woodin, R. L.; Beauchamp, J. L. *J. Am. Chem. Soc.* **1978**, *100*, 501. (b) Nicholas, J. B.; Pay, B. P.; Dixon, D. A. *J. Phys. Chem. A* **1999**, *103*, 1394.
(33) Cubero, E.; Luque, F. J.; Qrozco, M. *Proc. Natl. Acad. Sci. U.S.A.* **1998**, *95*, 5976.
(34) Ritchie, C. D.; Sager, W. F. *Prog. Phys. Org. Chem.* **1964**, *2*, 323.
(35) Hansch, C.; Leo, A.; Unger, S. H.; Kim, K. H.; Nikaitani, D.; Lien, E. J. *J. Med. Chem.* **1973**, *16*, 1207.
(36) Mecozzi, S.; West, A. P., Jr.; Dougherty, D. A. *J. Am. Chem. Soc.* **1996**, *118*, 2307.
(37) *Hyperchem6 and Hyperchem7.01* (trial version), Hypercube, Inc.: 1115 NW 4th Street, Gainesville, FL 32601, 1999, 2002.